

Discrete Limit Analysis for Framed Structures by using Hybrid-type Penalty Method

YAMAGUCHI, Kiyomichi / 竹内, 則雄 / 山口, 清道 / TAKEUCHI, Norio

---

(出版者 / Publisher)

法政大学情報メディア教育研究センター

(雑誌名 / Journal or Publication Title)

法政大学情報メディア教育研究センター研究報告

(巻 / Volume)

30

(開始ページ / Start Page)

1

(終了ページ / End Page)

11

(発行年 / Year)

2016-04-01

(URL)

<https://doi.org/10.15002/00013409>

## Discrete Limit Analysis for Framed Structures by using Hybrid-type Penalty Method

Kiyomichi Yamaguchi<sup>1)</sup> and Norio Takeuchi<sup>2)</sup>

<sup>1)</sup> Graduate School of Engineering and Design, Hosei University, Tokyo 162-0843, Japan,  
kiyomichi.yamaguchi.9r@stu.hosei.ac.jp

<sup>2)</sup> Department of Engineering and Design, Hosei University, Tokyo 162-0843, Japan, Takeuchi@hosei.ac.jp

### SUMMARY

In this study, bar elements for the hybrid-type penalty method (HPM) are developed. In this method for calculating the displacement field, it is assumed that an independent linear displacement field for the axial direction and an independent third-order displacement field for the bending of each element are combined. This model has six degrees of freedom: strain, gradient of strain, and the rigid-body displacement of the center of gravity of the elements. The continuity conditions of displacement are incorporated by using a penalty function. The elastic solution obtained with this method is consistent with the exact solution. The incremental loading method is used in the proposed discrete limit analysis. Because this method generates each plastic hinge sequentially, the progress of destruction can be followed. Accurate collapse loads and modes were obtained using numerical analysis.

KEY WORDS: hybrid-type penalty method; displacement field; bar elements; limit analysis; framed structures

### 1. INTRODUCTION

The analysis of framed structures is widely performed using the deformation method (DM). Because this method assumes a third-order displacement field, the elastic solution obtained by this method is consistent with the exact solution. Therefore, it is not necessary to develop a new analysis model for ordinary analysis of framed structures.

However, bar elements are used to model the rod material, the rock bolt into ground, or the reinforcement bars in reinforced concrete. In the case of a two-dimensional problem, the analysis model for reinforced concrete is composed of bar elements for reinforcement bars and a plate element for concrete. When considering the analysis of the progressive failure of reinforced concrete with the hybrid-type penalty method (HPM)<sup>1)</sup>, it is difficult to combine DM analysis of the bar element and HPM analysis of the plate element. The reason is that the displacement fields are different between DM and the HPM<sup>2)-4)</sup>; the degrees of freedom for DM are defined at nodal points, but the degrees of freedom for HPM are defined in elements.

In this study, bar elements for HPM are developed with the same displacement field and discretization method as the plane element. Additionally, we validated the results with the discrete limit analysis of framed structures<sup>5)6)</sup>.

### 2. HYBRID-TYPE VIRTUAL WORK EQUATION

Figure 1 shows the deformation of a beam material. In this case, using the equations of equilibrium, strain-displacement, and stress-strain, we can obtain the virtual work equation:

$$\int_{-l/2}^{l/2} \delta \varepsilon N dx + \int_{-l/2}^{l/2} \delta \chi M dx = \int_{-l/2}^{l/2} (\delta u \cdot q + \delta w \cdot p + \delta \theta \cdot m) dx \\ + (\delta u_a \bar{N}_a + \delta u_b \bar{N}_b) + (\delta w_a \bar{S}_a + \delta w_b \bar{S}_b) + (\delta \theta_a \bar{M}_a + \delta \theta_b \bar{M}_b) \quad (1)$$

where  $N(x)$  is the axial force;  $S(x)$  is the shear force;  $M(x)$  is the bending moment;  $p(x)$  is the axial distributed load;  $q(x)$  is the axial vertical distributed load;  $m(x)$  is the distributed moment;  $u$  and  $w$  is rigid displacement;  $\theta$  is the rigid rotation;  $\varepsilon$  is the axial strain;  $\chi$  is the curvature.

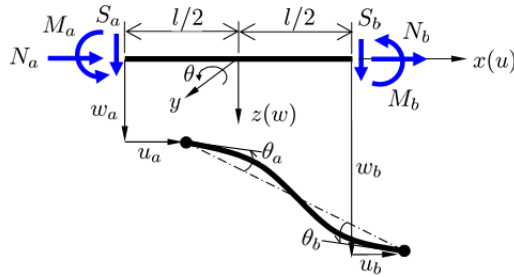


Fig.1 Degrees of freedom of beam material

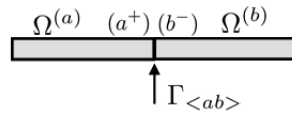


Fig. 2 Boundary  $\Gamma_{<ab>}$  between subdomains  $\Omega^{(a)}$  and  $\Omega^{(b)}$

Figure 2 shows  $\Gamma_{<ab>}$  as the common boundary between two domains  $\Omega^{(a)}$  and  $\Omega^{(b)}$ , which must have continuity of displacement. Therefore, the continuity condition of adjacent subdomains is denoted as

$$\mathbf{u}^{(a+)} = \mathbf{u}^{(b-)} \text{ on } \Gamma_{<ab>} \quad (2)$$

Eq.(2) introduces the continuity condition; the Lagrange multiplier for it is

$$H_{ab} \stackrel{\text{def.}}{=} \delta \int_{\Gamma_{<ab>}} \lambda \cdot (\mathbf{u}^{(b-)} - \mathbf{u}^{(a+)}) dS \quad (3)$$

From Eqs. (1) and (3), the hybrid-type virtual work equation is obtained:

$$\sum_{e=1}^M \left[ \int_{-l/2}^{l/2} \delta \varepsilon N dx + \int_{-l/2}^{l/2} \delta \chi M dx - \int_{-l/2}^{l/2} (\delta u \cdot q + \delta w \cdot p + \delta \theta \cdot m) dx - (\delta u_a \bar{N}_a + \delta u_b \bar{N}_b) - (\delta w_a \bar{S}_a + \delta w_b \bar{S}_b) - (\delta \theta_a \bar{M}_a + \delta \theta_b \bar{M}_b) \right] - \sum_{s=1}^N H_s = 0 \quad (4)$$

### 3. INTRODUCED DISCRETIZATION EQUATION

#### 3.1 Displacement Field

Figure 3 shows the displacement field of the bar element, where HPM is assumed to be third order. A way by Lee and Filippou<sup>5)</sup> is proposed as similar displacement field. The degree of freedom is the center of gravity of the element.

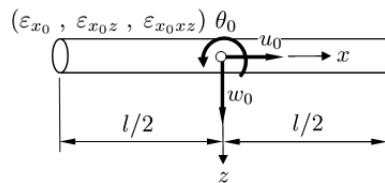


Fig. 3 Degrees of freedom for the bar element in the HPM

In Figure 3,  $u_0$  and  $w_0$  are rigid displacements;  $\theta_0$  is the rigid rotation;  $\varepsilon_{x_0}$  and  $\varepsilon_{x_0z}$ ,  $\varepsilon_{x_0zz}$  are the strain and its gradients, respectively. The displacement at an arbitrary point in the element is

$$\mathbf{u}^{(e)} = \mathbf{N}_d^{(e)} \mathbf{d}^{(e)} + \mathbf{N}_\varepsilon^{(e)} \boldsymbol{\varepsilon}^{(e)} = \mathbf{N}^{(e)} \mathbf{U}^{(e)} \quad (5)$$

$$\mathbf{u}^{(e)} = [u, w, \theta]^t, \quad \mathbf{d}^{(e)} = [u_0, w_0, \theta_0]^t, \quad \boldsymbol{\varepsilon}^{(e)} = [\varepsilon_{x_0}, \varepsilon_{x_0z}, \varepsilon_{x_0xz}]^t$$

$$\mathbf{N}_d^{(e)} = \begin{bmatrix} 1 & 0 & 0 \\ 0 & 1 & -x \\ 0 & 0 & 1 \end{bmatrix}, \quad \mathbf{N}_\varepsilon^{(e)} = \begin{bmatrix} x & 0 & 0 \\ 0 & -x^2/2 & -x^3/6 \\ 0 & x & x^2/2 \end{bmatrix}$$

$$\mathbf{N}^{(e)} = [ \mathbf{N}_d^{(e)} \quad \mathbf{N}_\varepsilon^{(e)} ], \quad \mathbf{U}^{(e)} = [ \mathbf{d}^{(e)} \quad \boldsymbol{\varepsilon}^{(e)} ]^t$$

Thus, the displacements at the end points are as follows:

$$\mathbf{u}^{(e^+)} = \mathbf{N}_d^{(e^+)} \mathbf{d}^{(e)} + \mathbf{N}_\varepsilon^{(e^+)} \boldsymbol{\varepsilon}^{(e)} = \mathbf{N}^{(e^+)} \mathbf{U}^{(e)} \quad (6)$$

$$\mathbf{u}^{(e^-)} = \mathbf{N}_d^{(e^-)} \mathbf{d}^{(e)} + \mathbf{N}_\varepsilon^{(e^-)} \boldsymbol{\varepsilon}^{(e)} = \mathbf{N}^{(e^-)} \mathbf{U}^{(e)} \quad (7)$$

Eqs. (6) and (7) are used at  $x = 1/2$  for  $(e^+)$  and at  $x = -1/2$  for  $(e^-)$  in Eq. (5). As above, the displacement field of HPM is defined for the degrees of freedom in the element. Therefore, independent displacement fields are assumed in each element.

### 3.2 Relative Displacement and Lagrange Multiplier

In the DM method, the degrees of freedom are defined at nodes, and the connection of adjacent elements is generally treated by having elements share nodes. However, the degrees of freedom for HPM are defined in the elements. Therefore, the methods are connected using the continuity condition. Figure 4 shows the relative displacement between two adjacent elements. Combining Eqs. (6) and (7) yields

$$\boldsymbol{\delta}_{\langle ab \rangle} = \mathbf{u}^{(b^-)} - \mathbf{u}^{(a^+)} = \mathbf{N}_{\langle ab \rangle} \mathbf{U}_{\langle ab \rangle} \quad (8)$$

where

$$\mathbf{N}_{\langle ab \rangle} = [ -\mathbf{N}^{(a^+)} \quad \mathbf{N}^{(b^-)} ], \quad \mathbf{U}_{\langle ab \rangle} = [ \mathbf{U}^{(a)} \quad \mathbf{U}^{(b)} ]^t$$

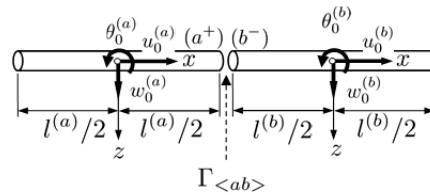


Fig. 4 Two adjacent elements

The Lagrange multiplier  $\lambda_{\langle ab \rangle}$  is the surface force (section force) on the boundary  $\Gamma_{\langle ab \rangle}$ . We define it using the relative displacement  $\boldsymbol{\delta}_{\langle ab \rangle}$  and the penalty function  $\mathbf{p}$  as follows.

$$\boldsymbol{\lambda}_{\langle ab \rangle} = \mathbf{p} \cdot \boldsymbol{\delta}_{\langle ab \rangle} \quad (9)$$

Writing Eq. (9) in its matrix form yields

$$\begin{Bmatrix} \lambda_{u\langle ab \rangle} \\ \lambda_{w\langle ab \rangle} \\ \lambda_{\theta\langle ab \rangle} \end{Bmatrix} = \begin{bmatrix} p_u & 0 & 0 \\ 0 & p_w & 0 \\ 0 & 0 & p_\theta \end{bmatrix} \begin{Bmatrix} \delta_{u\langle ab \rangle} \\ \delta_{w\langle ab \rangle} \\ \delta_{\theta\langle ab \rangle} \end{Bmatrix} \quad (10)$$

where  $p_u$ ,  $p_w$ , and  $p_\theta$  are penalty functions. By using a sufficiently large penalty function, the continuity of displacement on the boundary  $\Gamma_{\langle ab \rangle}$  is maintained.

### 3.3 Discretization Equation

By combining Eqs. (5) through (10) of the discretization equation, an equation of hybrid-type virtual work like Eq. (4) can be obtained; furthermore, it can be written in a form compatible with HPM. The equation of virtual work is

$$\delta W^{(e)} = \delta \mathbf{U} \mathbf{D}^{(e)} \mathbf{U} - \delta \mathbf{U} \mathbf{P}_f^{(e)} - \delta \mathbf{U} \mathbf{P}_M^{(e)} \quad (11)$$

The continuity condition is

$$\delta H_{\langle s \rangle} = -\delta \mathbf{U}^t \mathbf{K}_{\langle s \rangle} \mathbf{U} \quad (12)$$

Therefore, the equation of hybrid-type virtual work is

$$\delta \mathbf{U}^t \left( \sum_{e=1}^M \mathbf{D}^{(e)} + \sum_{s=1}^N \mathbf{K}_{\langle s \rangle} \right) \mathbf{U} - \delta \mathbf{U}^t \sum_{e=1}^M \left( \mathbf{P}_M^{(e)} + \mathbf{P}_f^{(e)} \right) = 0 \quad (13)$$

Finally, by assuming an arbitrary non-trivial value for the virtual displacement  $\delta \mathbf{U}$ , the discretization equation can be obtained:

$$\mathbf{K} \mathbf{U} = \mathbf{P} \quad (14)$$

where

$$\mathbf{K} = \sum_{e=1}^M \mathbf{D}^{(e)} + \sum_{s=1}^N \mathbf{K}_{\langle s \rangle}$$

And

$$\mathbf{P} = \sum_{e=1}^M \left( \mathbf{P}_f^{(e)} + \mathbf{P}_M^{(e)} \right)$$

#### 4. PIN ELEMENT

##### 4.1 Discretization Equation

###### (1) Linearly Connecting Bar

In the case of linearly connecting bar elements as in Figure 4, the coefficient matrix  $\mathbf{K}$  is as follows:

$$\mathbf{K}^{(a)} + \mathbf{K}^{(b)} + \mathbf{K}_{\langle ab \rangle} = \begin{bmatrix} {}^t \mathbf{N}^{(a^+)} \mathbf{p} \mathbf{N}^{(a^+)} + \mathbf{E}^{(a)} & -{}^t \mathbf{N}^{(a^+)} \mathbf{p} \mathbf{N}^{(b^-)} \\ -{}^t \mathbf{N}^{(b^-)} \mathbf{p} \mathbf{N}^{(a^+)} & {}^t \mathbf{N}^{(b^-)} \mathbf{p} \mathbf{N}^{(b^-)} + \mathbf{E}^{(b)} \end{bmatrix} \quad (15)$$

where

$$\mathbf{E}^{(e)} = \begin{bmatrix} 0 & 0 & 0 & 0 & 0 & 0 \\ 0 & 0 & 0 & 0 & 0 & 0 \\ 0 & 0 & 0 & 0 & 0 & 0 \\ 0 & 0 & 0 & EA & 0 & 0 \\ 0 & 0 & 0 & 0 & EI & 0 \\ 0 & 0 & 0 & 0 & 0 & EI l^3 / 12 \end{bmatrix}$$

However, adjacent rod materials are mostly connected at angles, and the displacement field of HPM is defined for the degrees of freedom in the bar element. Therefore, it is necessary to include information on the connecting angles into the coefficient matrix of Eq. (15).

###### (2) Pin Element Connected to the End

Figure 5 shows how we develop pin elements that do not have length and mass. In the case of a two-dimensional problem, there are three degrees of freedom for the pin element: rigid displacement and rigid rotation.

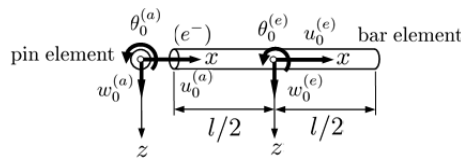


Fig. 5 Degrees of freedom for a pin element connected to the left-end

At the left-end of bar element "a", the relative displacement between the pin element and the bar element is represented as follows.

$$\delta_{\langle ae \rangle} = \begin{bmatrix} -\mathbf{I} & \mathbf{N}^{(e^-)} \end{bmatrix} \begin{Bmatrix} \mathbf{d}^{(a)} \\ \mathbf{U}^{(e)} \end{Bmatrix} \quad (16)$$

where  $\mathbf{I}$  is an identity matrix. The continuity condition is

$$\mathbf{K}_{\langle ae \rangle} \mathbf{U}_{\langle ae \rangle} = \begin{Bmatrix} -\mathbf{I} \\ {}^t \mathbf{N}^{(e^-)} \end{Bmatrix} \mathbf{p} \begin{bmatrix} -\mathbf{I} & \mathbf{N}^{(e^-)} \end{bmatrix} \begin{Bmatrix} \mathbf{d}^{(a)} \\ \mathbf{U}^{(e)} \end{Bmatrix} \quad (17)$$

The element stiffness matrix is the sum

$$\mathbf{K}^{(e)} \mathbf{U}^{(e)} = \mathbf{E}^{(e)} \mathbf{U}^{(e)} \quad (18)$$

Therefore, the coefficient matrix with a pin on the left-end is as follows:

$$\mathbf{K}^{(e)} \mathbf{U}^{(e)} + \mathbf{K}_{\langle ae \rangle} \mathbf{U}_{\langle ae \rangle} = \begin{bmatrix} \mathbf{p} & -\mathbf{p} \mathbf{N}^{(e^-)} \\ -{}^t \mathbf{N}^{(e^-)} \mathbf{p} & {}^t \mathbf{N}^{(e^-)} \mathbf{p} \mathbf{N}^{(e^-)} + \mathbf{E}^{(e)} \end{bmatrix} \begin{Bmatrix} \mathbf{d}^{(a)} \\ \mathbf{U}^{(e)} \end{Bmatrix} \quad (19)$$

Similarly, in the case where the pin element is at the right-end of bar element "b", as in Figure 6, the coefficient matrix is

$$\mathbf{K}^{(e)} \mathbf{U}^{(e)} + \mathbf{K}_{\langle be \rangle} \mathbf{U}_{\langle be \rangle} = \begin{bmatrix} \mathbf{p} & -\mathbf{p} \mathbf{N}^{(e^+)} \\ -{}^t \mathbf{N}^{(e^+)} \mathbf{p} & {}^t \mathbf{N}^{(e^+)} \mathbf{p} \mathbf{N}^{(e^+)} + \mathbf{E}^{(e)} \end{bmatrix} \begin{Bmatrix} \mathbf{d}^{(b)} \\ \mathbf{U}^{(e)} \end{Bmatrix} \quad (20)$$

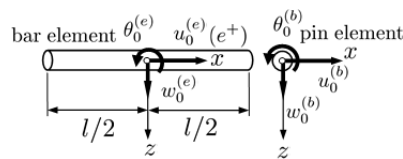


Fig. 6 Degrees of freedom for a pin element connected to the right-end

#### 4.2 Coordinate Transformation

In Figure 7, we consider the case of a connecting pin element between two bar elements.

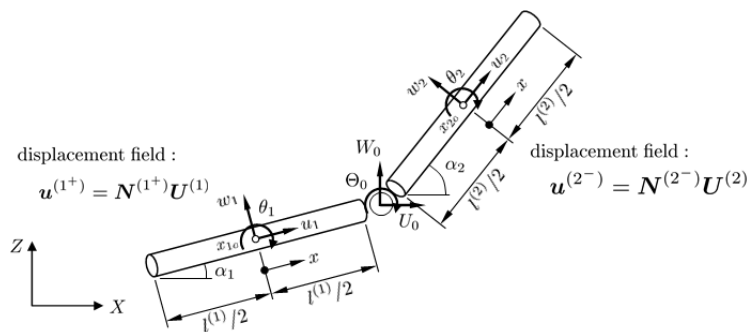


Fig. 7 Local coordinate system and global coordinate system

First, we consider the bar element "1" on the left side of the pin element. The displacement of the pin element has transformed the coordinates of the local coordinate system of bar element "1" as

$$\mathbf{d}^{(0_1)} = \mathbf{r}^{(1)} \mathbf{d}^{(1)} \quad (21)$$

Writing Eq. (21) in its matrix form yields

$$\begin{Bmatrix} u_{01} \\ W_{01} \\ \theta_{01} \end{Bmatrix} = \begin{bmatrix} \cos \alpha_1 & \sin \alpha_1 & 0 \\ -\sin \alpha_1 & \cos \alpha_1 & 0 \\ 0 & 0 & 1 \end{bmatrix} \begin{Bmatrix} U_0 \\ W_0 \\ \Theta_0 \end{Bmatrix} \quad (22)$$

Thus, the coefficient matrix corresponding to Eq. (19) becomes

$$\mathbf{K}^{(1)} \mathbf{U}^{(1)} + \mathbf{K}_{\langle 01 \rangle} \mathbf{U}_{\langle 01 \rangle} = \begin{bmatrix} {}^t \mathbf{r}^{(1)} \mathbf{p} \mathbf{r}^{(1)} & -{}^t \mathbf{r}^{(1)} \mathbf{p} \mathbf{N}^{(1^+)} \\ -{}^t \mathbf{N}^{(1^+)} \mathbf{p} \mathbf{r}^{(1)} & {}^t \mathbf{N}^{(1^+)} \mathbf{p} \mathbf{N}^{(1^+)} + \mathbf{E}^{(1)} \end{bmatrix} \begin{Bmatrix} \mathbf{d}^{(0)} \\ \mathbf{U}^{(1)} \end{Bmatrix} \quad (23)$$

Next, we consider the bar element "2" on the right side of the pin element. The displacement of the pin element has transformed the coordinates of the local coordinate system of bar element "2" as

$$\mathbf{d}^{(0_2)} = \mathbf{r}^{(2)} \mathbf{d}^{(0)} \quad (24)$$

Writing Eq. (24) in its matrix form yields

$$\begin{Bmatrix} u_{02} \\ W_{02} \\ \theta_{02} \end{Bmatrix} = \begin{bmatrix} \cos \alpha_2 & \sin \alpha_2 & 0 \\ -\sin \alpha_2 & \sin \alpha_2 & 0 \\ 0 & 0 & 1 \end{bmatrix} \begin{Bmatrix} U_0 \\ W_0 \\ \Theta_0 \end{Bmatrix} \quad (25)$$

Similarly, the coefficient matrix corresponding to Eq. (20) becomes

$$\mathbf{K}^{(2)} \mathbf{U}^{(2)} + \mathbf{K}_{<02>} \mathbf{U}_{<02>} = \left[ \begin{array}{c|c} {}^t \mathbf{r}^{(2)} \mathbf{p} \mathbf{r}^{(2)} & -{}^t \mathbf{r}^{(2)} \mathbf{p} \mathbf{N}^{(2+)} \\ \hline -{}^t \mathbf{N}^{(2+)} \mathbf{p} \mathbf{r}^{(2)} & {}^t \mathbf{N}^{(2+)} \mathbf{p} \mathbf{N}^{(2+)} + \mathbf{E}^{(2)} \end{array} \right] \begin{Bmatrix} \mathbf{d}^{(0)} \\ \mathbf{U}^{(2)} \end{Bmatrix} \quad (26)$$

## 5. NUMERICAL EXAMPLE

### 5.1 Material Nonlinear Analysis

In discrete limit analysis, the failure condition of a bar model has following forms:

$$f(M) = \left( \frac{M_n}{M_y} \right)^2 - 1 \quad (27)$$

where  $M_y$  is a plastic bending moment. If a plastic hinge will occur, the bending moment on intersection boundary is assumed to be zero:

$$f(M) = 0 \quad (28)$$

For this case, we can obtain incremental bending moment as follows:

$$\Delta M_n = k^{(p)} \Delta \delta \quad (29)$$

From Eq. (29), the penalty function is

$$k_{ij}^{(p)} = k_i^{(e)} \delta_{ij} - \frac{1}{\sum k_i^{(e)} f_i^2} f_i f_j k_i^{(e)} k_j^{(e)} \quad (30)$$

Load at the  $(i + 1) - th$  step can be calculated by using the load at the  $i - th$  step:

$$\mathbf{P}^{(i+1)} = (1 - r_i) \mathbf{P}^i \quad (31)$$

where  $r_i$  is a rate of load increment which we can calculate using this equation:

$$f(M_n + r \cdot \Delta M_n) = 0 \quad (32)$$

After solving following equation:

$$\left( \frac{M_n + r \cdot \Delta M_n}{M_y} \right)^2 - 1 = 0 \quad (33)$$

We will obtain  $r$ :

$$r = \frac{M_y + M_n}{\Delta M_n} \quad (34)$$

In case of bending moment, residual load at the  $n - th$  step will be:

$$\mathbf{P}^{(n)} = \prod_{i=0}^{n-1} [(1 - r_i)] \Delta \mathbf{P} \quad (35)$$

Cumulative rate of increment is as follows:

$$r_{TOTAL} = \sum_{k=1}^n \left( \prod_{i=0}^{k-1} [(1 - r_i)] \right) r_k \quad (36)$$

When  $t_{TOTAL}$ , iteration is finish.

### 5.2 Example of a Single-Story Rigid Frame Structure

Figure 9 shows a single-story rigid frame structure with fixed ends, acted upon by a horizontal load. The even-numbered elements are bar elements, and the odd-numbered elements are pin elements. The horizontal load is applied to pin element number 3. Material properties show in Table 1.

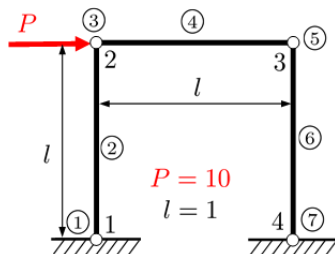


Fig. 9 Example single-story rigid frame structure

Table 1 Material properties

Elastic modulus E	100
Elastic shear modulus G	76.923
Cross-sectional area A	1
Moment of inertia of area I	1
Plastic bending moment $M_y$	1

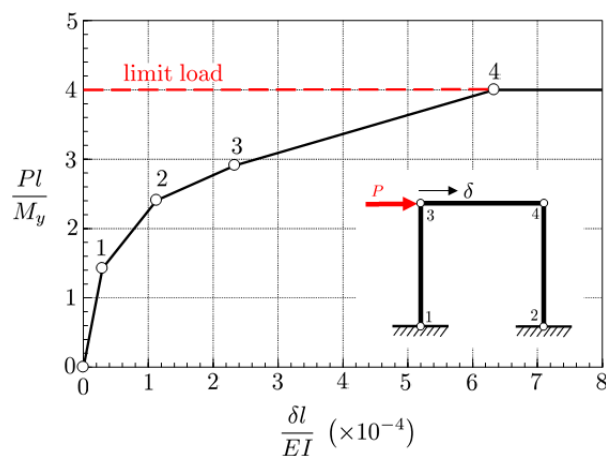


Fig. 10 Load-displacement curve and the sequence of generated plastic hinges

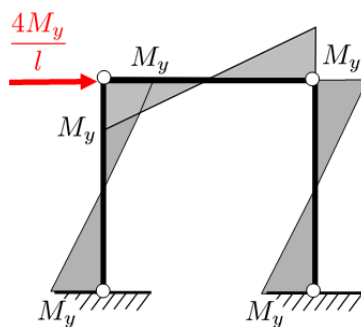


Fig. 11 shows bending moment at collapse.

Figure 10 shows the load-displacement curve for this example. The break points in the graph denote the generation of plastic hinges. In the figure of the model, the number is the order in which they occur.

The resulting collapse from the loading and the generated plastic hinge points match the theoretical solution. Figure 11 shows bending moment at collapse.



5.3 Example of a two-Story Rigid Frame Structure

Figure 12 shows a two-story rigid frame structure with fixed ends, acted upon by a horizontal load. The even-numbered elements are bar elements, and the odd-numbered elements are pin elements. The horizontal loads are applied to pin elements number 3 and 9. Material properties show in Table 2.

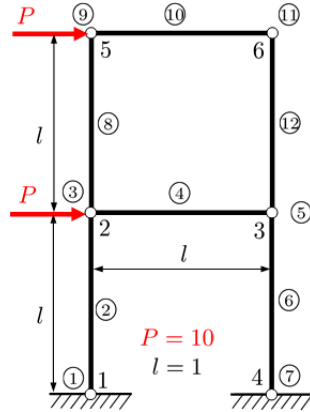


Fig. 12 Example two-story rigid frame structure

Table 2 Material properties

Elastic modulus E		100
Elastic shear modulus G		76.923
Cross-sectional area A		1
Moment of inertia of area I		1
Plastic bending moment $M_y$	Pillars ((2)(6)(8)(12))	2
	Beams ((4)(10))	1

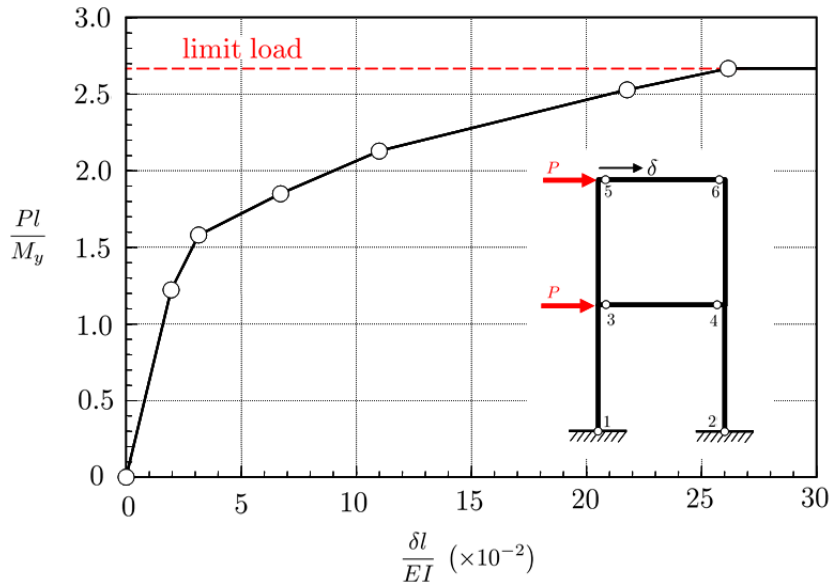


Fig. 13 Load-displacement curve and the sequence of generated plastic hinges

Figure 13 shows the load-displacement curve for this example.

The resulting collapse from the loading and the generated plastic hinge points match the theoretical solution. Figure 14 shows bending moment at collapse.

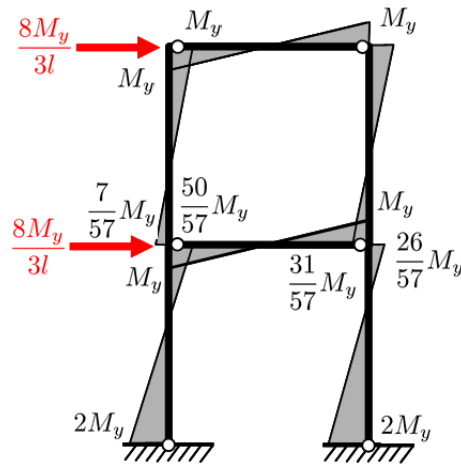


Fig. 14 Bending moment at the collapse

5.4 Example of a two-Story Rigid Frame Structure with Horizontal and Vertical Loads

Figure 15 shows a two-story rigid frame structure with, acted upon by horizontal and vertical loads. The even-numbered elements are bar elements, and the odd-numbered elements are pin elements. The horizontal loads are applied to pin elements number 3 and 11. The vertical loads are applied to beam elements number 5 and 13. Material properties show in Table 3.

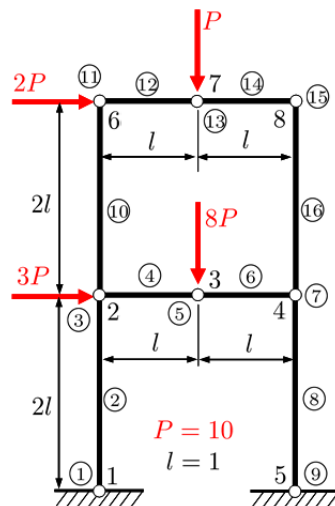


Fig. 15 The example two-story rigid frame structure with horizontal and vertical loads

Table 3 Material properties

Elastic modulus E		100
Elastic shear modulus G		76.923
Cross-sectional area A		1
Moment of inertia of area I		1
Plastic bending moment $M_y$	Pillars and beams of first story ((2)(4)(6)(8))	3.0
	Pillars of second story ((10)(16))	1.5
	Beams of second story ((12)(14))	2.0

Figure 16 shows the load-displacement curve for this example.

The resulting collapse from the loading and the generated plastic hinge points match the theoretical solution. Figure 17 shows bending moment at collapse.

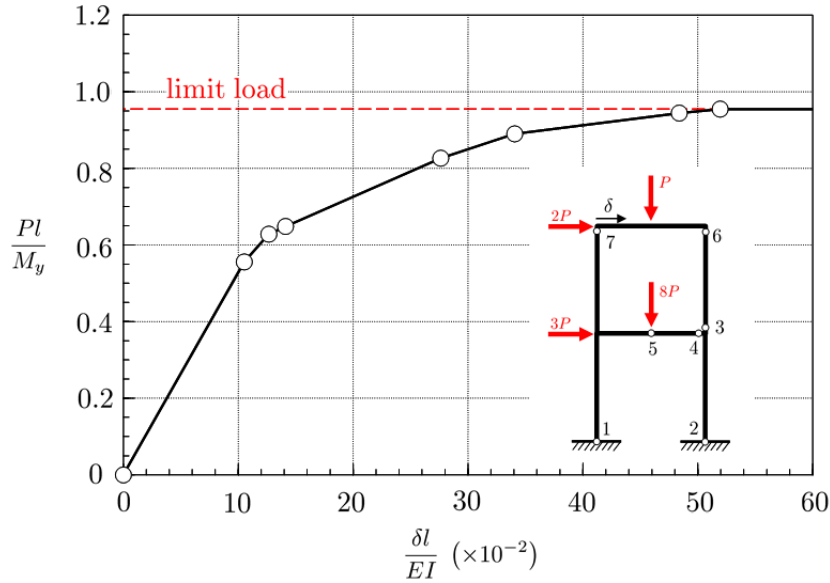


Fig. 16 Load-displacement curve and the sequence of generated plastic hinges

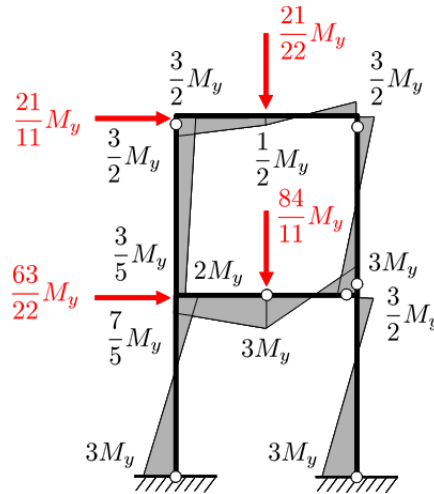


Fig. 17 Bending moment at collapse

6. CONCLUSIONS

In this study, bar elements for the hybrid-type penalty method were developed with the same discretization as the plate element. In this method for computing the displacement field, it is assumed that an independent linear displacement field for the axial direction and an independent third-order displacement field for the bending of each element are combined. Therefore, there are six degrees of freedom, which is the same of number as for the ordinary displacement method. With a sufficiently large penalty function, the continuity of displacement is retained on the boundary, and the obtained displacement solution is the same as that obtained from the displacement method.

When the bar elements are connected at angles, a pin element is used to consider the coordinate transformation. There are three degrees of freedom for each pin element: rigid displacement and rigid rotation on global coordinate system.

In the proposed discrete limit analysis, nonlinear material properties are used for plastic hinges, and the load incremental method is used. Validating the method with rigid frame structures with fixed ends, accurate collapse loads and modes are obtained, matching the theoretical solutions.

Therefore, the new bar element for HPM is validated, and we expect that the proposed method can be combined with the plate element in the progressive discrete analysis of HPM.

## REFERENCES

- [1] Fujiwara, Y., Takeuchi, N., Shiomi, T. and Kambayashi A., Discrete crack modeling of RC structure using hybrid-type penalty method, *Int. J. Aerospace and Lightweight Structures*, **3**(2), 263-275 (2013)
- [2] Takeuchi, N., Kusabuka, M., Takeda, H., Sato, K. and Kawai, T., The discrete limit analysis by using the hybrid model with the penalty, *J. Struct. Eng.* **46A**, 261-270 (2000)
- [3] Takeuchi, N., Ohki, H., Kanbayashi, A. and Kusabuka, M., Material non-linear analysis by using discrete model applied penalty method in hybrid displacement model, *Trans. JSCEs*, **2001**, Paper no. 20010002, 1-10 (2001)
- [4] Takeuchi, N., Tajiri, Y. and Hamasaki, H., Development of modified RBSM for rock mechanics using principle of hybrid-type virtual work, *Analysis of Discontinuous Deformation: New Developments and Applications* (CRC Press, London, UK), 395-403 (2009)
- [5] Lee, C. L. and Filippou, F. C., Frame elements with mixed formulation for singular section response, *Int. J. Numer. Meth. Engng*, **78**, 1320-1344(2009)
- [6] Lynn, K., M. and Isobe, D., Finite element code for impact collapse problems of framed structures, *Int. J. Numer. Meth. Engng.*, **69**, 2538-2563(2007)